Renewable Energy 97 (2016) 823–837

Contents lists available at ScienceDirect

Renewable Energy

journal homepage: www.elsevier.com/locate/renene

Parameter extraction of solar cell models based on adaptive differential evolution algorithm

C. Chellaswamy [a,*], R. Ramesh [b]

[a] St.Peter's University, St.Peter's Institute of Higher Education and Research, Chennai, India
[b] Department of Electronics and Communication Engineering, Saveetha Engineering College, Chennai, India

ARTICLE INFO

Article history:
Received 13 August 2015
Received in revised form
27 May 2016
Accepted 8 June 2016
Available online 23 June 2016

Keywords:
Modeling
Optimization algorithm
Parameter extraction
Photovoltaic
Differential evolution technique

ABSTRACT

In this paper, a new approach based on adaptive Differential Evolution Technique (DET) is used to extract the parameters of solar cell models accurately. The adaption is achieved through crossover and mutation factor. It is indicated that the optimization with an objective function can minimize the difference between the estimated and measured values. In order to verify the performance of the proposed system, three different solar cell models: single diode model, double diode model, and photovoltaic module are used to extract the parameters. The analysis is performed by using the voltage and current data sets. The result shows that the proposed DET outperforms these other methods: chaos particle swarm optimization (CPSO), genetic algorithm (GA), harmony search algorithm (HSA), and artificial bee swarm optimization (ABSO). Furthermore, the DET technique is practically validated by two different solar cell types such as monocrystalline and multi-crystalline and modules. The performance of solar cell models has been verified and the outcome shows that it is an optimal method which suits the parameter extraction of solar cells and modules.

1. Introduction

Renewable energy sources such as photovoltaic (PV) and wind energy have shown significant growth over the last few decades. In particular, solar energy is promising renewable technologies due to ease of installation, very low maintenance, readily available in nature, and without pollution [1]. Renewable sources produce local heat even though the thermal reduction is achieved by avoiding CO_2 emission. The PV panels are dark and they absorb approximately 85% of incoming light whereas 15% is used to generate electricity. The remaining 70% will produce heat [2]. Various investigations on PV systems have become popular due to its significance in the past few years. However, a proper system design is also required for increasing the overall efficiency [3,4]. Several models have been introduced to analyze the above study, among the models: single diode and double diode models are the most popular [5]. In these models, the latter one is preferable because the physical module and its I-V characteristics closely resemble each other, but it has a wide range of computations [6].

There are two possible approaches such as analytical solution method and numerical method that have been developed for extracting various parameters of solar modules [7,8]. The analytical method requires different key points for I-V characteristics such as a current and a voltage at the maximum power point, open circuit voltage, short circuit current and the slope of I-V curve. It is noted that the I-V characteristic is greatly non-linear and the parameters vary dependent on the environmental conditions due to parameter changes, which leads to significant errors in the computed parameters [9]. The numerical method is more accurate than the analytical method because it is based on a certain algorithm to fit the points on the I-V curve [10]. However, the algorithm requires more computation and the accuracy depends on the cost function and the type of fitting algorithm.

Optimization and metaheuristics algorithms are widely used in parameter extraction of solar cells. Evolutionary algorithms are the natural choice for parameter extraction problems because they are capable of replacing the standard test condition. Evolution algorithm methods are preferred to solve parameter extraction regardless of gradient and information of initial conditions [11]. Various evolutionary algorithms such as genetic algorithm (GA) [12,13], particle swarm optimization (PSO) [14], simulated annealing (SA) [15] have been included in parameter extraction for solar

* Corresponding author.
E-mail addresses: chella_info@yahoo.co.in (C. Chellaswamy), ramesh@saveetha.ac.in (R. Ramesh).

http://dx.doi.org/10.1016/j.renene.2016.06.024
0960-1481/

Nomenclature

L_i	length of individual
D	p-n junction of solar cell
I_t	terminal current
k_{max}	maximum number of generation
M	number of real I-V data
m	ideality factor of the diode
R_{ser}	series resistance
q	charge of electron (1.602×10^{-19} C)
T_c	cell temperature
I_i	illuminated cell current
I_m	current of PV module
I_{ph}	cell-generated photocurrent
I_s	shaded cell current
V_s	shaded cell voltage
P_s	power dissipated by shaded cell
I_{es}	estimated cell current
C_r	crossover probability constant
F	mutation factor
k	Boltzmann constant (1.381×10^{-23} J/K)
NP	size of population
D_k	blocking diode
R_{sh}	shunt resistance
RC	rate of crossover
D_b	bypass diode
I_d	diode current
V_m	voltage of PV module
V_T	thermal voltage
V_t	terminal voltage
I_{sd}	reverse saturation current of diode
I_{sh}	shunt resistor current
I_{me}	measured cell current
Subscript	
1,2	first and second

cells. The electrical characteristics of solar cells and parameter extraction using GA are computed from the maximum power point [16]. The PSO technique is used to extract various parameters of the PV module [17,18]. The modified differential evolution algorithm called penalty based DE algorithm is used to extract various parameters of solar cells [19].

GA has limitations like low speed and degradation [20]. The trade-off between temperature, cooling schedule and inconsistencies are the major issues making SA less suitable for parameter extraction problems [21]. To improve the consistency of the estimation, PSO is introduced in conjunction with cluster analysis. The PSO is also used to estimate the parameters and the cluster analysis for filtering the non-feasible solution [22,23]. This increases the consistency and reliability, even though it requires all previous points to be stored. It increases the computational burden and therefore the simulation speed will be greatly impacted. The searching space of the parameters should be broadened to avoid convergence problems and the extraction processes satisfy different boundary conditions. A fast and accurate two-diode model for photovoltaic modules has been studied by Ishaque et al. [24]. The control parameters are changed randomly in to a self-adaptive evolutionary algorithm so that the convergence is difficult and the selection process has not been impacted by the evolution [25,26]. To increase the efficiency of the control parameters such as F and RC, an adaptive algorithm has been introduced [27]. Differential evolution using adaptive methods have been studied by Tvrdik using a numerical comparison [28].

Unlike conventional differential evolution (DE), the solution of adaptive DE is always in the feasible region and unconstrained in nature. Therefore, it is reliable to include the adaptive DE. As a result, a greater number of solutions will be created. The solution takes part in the evolution process and in the accuracy of the method, where diversity and consistency will be improved. In this work, the performance of DET is investigated for individual solar cells in each module parameter extraction process and is compared with four methods namely GA, CPSO, HAS, and ABSO. Finally, to ensure the practical use of the proposed DET method, it is validated by two different solar cells and modules such as monocrystalline (SM55) and multi-crystalline (KG200GT). The remnants of this paper is organized in the following ways: section 2 describes the problem formulation of parameter extraction with single diode model, double diode model, and model of PV module; section 3 describes the DE and adaptive DE algorithm; section 4 explains the simulation and experimental results; and the conclusion is discussed in section 5.

2. Problem formulation

The main objective of the parameter extraction for solar cell models is to minimize the difference between measured and simulated current. Two circuit models (single and double diode) are typically used to describe the performance of solar cells. The single diode model provides better performance under normal operating condition, but the performance is very less at low irradiance [29]. On the other hand, the two diode model modifies the current equation by including the recombination losses in space-charges by incorporating an additional diode.

2.1. Single diode model

The equivalent circuit model of a solar cell using single diode model is shown in Fig. 1. In Fig. 1, the index D, R_{sh}, R_{ser}, and I_{ph} represents the p-n junction of a solar cell, shunt resistance, series resistance, and photocurrent due to solar irradiation respectively. The diffusion current, diode ideality factor, and recombination currents are combined together in the single diode model. The governing equation for this equivalent circuit is formulated using Kirchoff's current law for current I_t and it is given as:

$$I_t = I_{ph} - I_d - I_{sh} \tag{1}$$

In single diode model, I_d is modeled using Shockley equation,

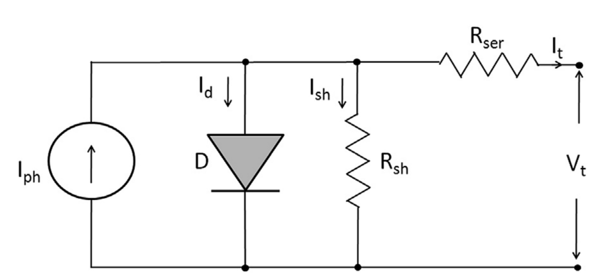

Fig. 1. Equivalent circuit model of solar cell using single diode model.

$I_d = I_{sd}[\exp(V_t + I_t R_{ser})/mV_T] - 1$, the thermal voltage $V_T = kT_c/q$ and the shunt current $I_{sh} = (V_t + I_t R_{ser})/R_{sh}$.

Now (1) can be represented by Shockley equation and written as [30]:

$$I_t = I_{ph} - I_{sd}\left[\exp\left(\frac{q(V_t + R_{ser}I_t)}{mkT_c}\right) - 1\right] - \left(\frac{V_t + R_{ser}I_t}{R_{sh}}\right) \tag{2}$$

Five parameters such as series resistance (R_{ser}), shunt resistance (R_{sh}), reverse saturation current of the diode (I_{sd}), photovoltaic current (I_{ph}), and ideality factor of the diode (m) can be extracted from the given set of I-V data.

2.2. Double diode model

The equivalent circuit model of a solar cell using double diode model is shown in Fig. 2. The governing equation for this equivalent circuit is formulated using Kirchoff's current law for current I_t and it is given as:

$$I_t = I_{ph} - I_{d1} - I_{d2} - I_{sh} \tag{3}$$

In double diode model, I_{d1}, I_{d2} can be modeled using Shockley equation as:

$$I_{d1} = I_{sd1}\left[\exp\left(\frac{V_t + I_t R_{ser}}{m_1 V_T}\right) - 1\right] \tag{4}$$

$$I_{d2} = I_{sd2}\left[\exp\left(\frac{V_t + I_t R_{ser}}{m_2 V_T}\right) - 1\right] \tag{5}$$

Now substitute I_{d1}, I_{d2} and I_{sh} in (3) and can be written as [31]:

$$I_t = I_{ph} - I_{sd1}\left[\exp\left(\frac{q(V_t + R_{ser}I_t)}{m_1 kT_c}\right) - 1\right] - I_{sd2}\left[\exp\left(\frac{q(V_t + R_{ser}I_t)}{m_2 kT_c}\right) - 1\right] - \left(\frac{V_t + R_{ser}I_t}{R_{sh}}\right) \tag{6}$$

Seven parameters such as series resistance, shunt resistance, photovoltaic current, the saturation current (I_{sd1} and I_{sd2}) and ideality factor (m_1 and m_2) of a diode can be extracted from the given set of I-V data.

2.3. Model of PV module

Fig. 3 shows the connection schematic of the solar cells in the module with a bypass diode. Assume that all the solar cells are identical under uniform irradiance and temperature. The commercial solar cell modules are a serial connection of several cells [32,33].

Using Kirchoff's current law, the I-V curve equation is derived as follows:

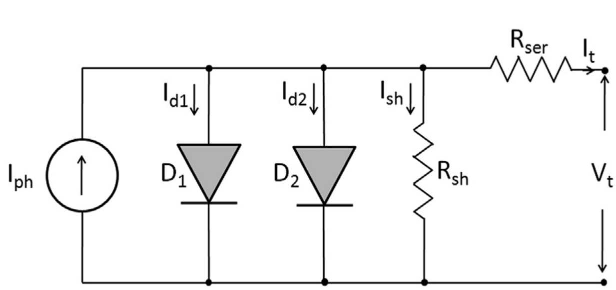

Fig. 2. Equivalent circuit model of solar cell using double diode model.

$$I_t = I_{ph} - I_{sd}\left[\exp\left(\frac{q(V_t + R_{ser}I_t)}{N_s mkT_c}\right) - 1\right] - \left(\frac{V_t + R_{ser}I_t}{R_{sh}}\right) \tag{7}$$

where I_t and N_s represent the terminal current and number of solar cells connected in series in the module respectively.

2.4. Solar cell model optimization problem

The solar cell model parameter extraction is an optimization process which minimizes the difference between real and estimated values. The parameter estimation using optimization technique is implemented in the following approach:

- a set of real data of I-V for a solar cell or a PV module is measured.
- an objective function is defined for minimizing the difference between the real data and measured values.
- the parameters are tuned by applying an optimization algorithm until the best objective function is obtained.
- after completing the optimization algorithm, the optimal value is extracted from the solution obtained by the optimization algorithm.

Now assign a vector U, for each value, which is extracted from the optimization algorithm. The parameter vector for the single diode model is U = [R_{ser}, R_{sh}, I_{sh}, I_{sd}, m] and for the double diode model U = [R_{ser}, R_{sh}, I_{sh}, I_{sd1}, I_{sd2}, m_1, m_2]. An objective function needs to be defined in the optimization problem and the corresponding function for solar model parameter extraction can be defined from (2), (6) and (7). The homogeneous equations for the corresponding equations are given as:

$$f(V_t,\ I_t, U) = I_t - I_{ph} + I_{sd}\left[\exp\left(\frac{q(V_t + R_{ser}I_t)}{mkT_c}\right) - 1\right] + \left(\frac{V_t + R_{ser}I_t}{R_{sh}}\right) \tag{8}$$

$$f(V_t,\ I_t, U) = I_t - I_{ph} + I_{sd1}\left[\exp\left(\frac{q(V_t + R_{ser}I_t)}{m_1 kT_c}\right) - 1\right] + I_{sd2}\left[\exp\left(\frac{q(V_t + R_{ser}I_t)}{m_2 kT_c}\right) - 1\right] + \left(\frac{V_t + R_{ser}I_t}{R_{sh}}\right) \tag{9}$$

$$f(V_t,\ I_t, U) = I_t - I_{ph} - I_{sd}\left[\exp\left(\frac{q(V_t + R_{ser}I_t)}{N_s mkT_c}\right) - 1\right] - \left(\frac{V_t + R_{ser}I_t}{R_{sh}}\right) \tag{10}$$

Now the values of U can be substituted into (8)–(10), the solution $f(V_t, I_t, U)$ for each pair of I-V data are mostly different. The difference between real and estimated data can be evaluated, typically by the root mean square error (RMSE) criterion. For parameter extraction of solar cell models, the following function is used to minimize the RMSE as:

$$\mathit{minimize\ RMSE} = \sqrt{\frac{1}{M}\sum_{i=1}^{M} f(V_t,\ I_t, U)^2} \tag{11}$$

where M is the number of real I-V data and the output of RMSE guide the optimization search for the better value of the vector U. If the value of RMSE is bad, the optimization algorithm tuned to the vector U and it is substituted back into (8)–(10). This iterative

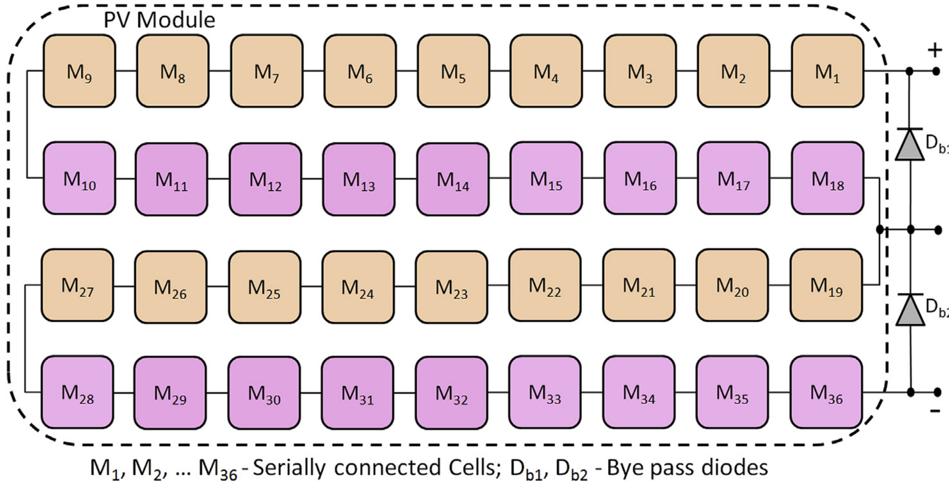

Fig. 3. Connection schematic of the solar cells in the module with bypass diode.

procedure improves the value of vector U and stops if the output value is good enough or the optimization algorithm attains maximum iteration time.

3. Differential evolution algorithm

Differential evolution is a heuristic, population-based algorithm originally proposed by Storn and Price in 1997 [34]. DE is a search and optimization technique, which generates new vectors by adding the third one with the difference of two population vectors. There are several variants of DE and it can be expressed as:

$$DE/mu/dv/cr \tag{12}$$

where mu, dv and cr represent the mutated vector, a number of difference vector, and crossover scheme respectively. DE has different advantages such as simplicity, robustness, requiring few control parameters and effectiveness. It can also work with multi-dimensional, noisy and time-dependent objective functions [35]. Based on these advantages, we choose DE for optimization parameter estimation problem.

3.1. DE-based optimal parameter estimation

Consider the solar cell model parameter optimization as (11), U is the decision variable which contains n variables $x_i \in R^n$. The step-by-step procedure for implementing DE algorithm is described as follows:

Step 1. The population (NP) of Q-dimensional parameter vector U_i^k and the population of solution P^k, $P_u^k = U_i^k$, i = 1,2, …,NP; k = 1,2, …,k_{max} and $U_i^k = U_{j,i}^k$, j = 1,2, …,Q.

The index i represent the population index, j represents the parameters within the vectors and k is the generation to which a vector belongs.

The population NP has Q-dimensional vectors $U_i^k = [U_{1,i}^k,\ U_{2,i}^k,\ \ldots, U_{j,i}^k, \ldots,\ U_{Q,i}^k]$. Each vector forms a candidate solution to the Q-dimensional optimization problem and values are randomly selected within the interval U_L and U_M. $U_L = [U_{1,L}, U_{2,L}, \ldots,\ U_{Q,L}]$ and $U_M = [U_{1,M}, U_{2,M}, \ldots,\ U_{Q,M}]$ are the lower and upper limits of the search space respectively. Now, the initial population in the search space is given by:

$$U_{j,i}^1 = U_L + rand(0,1)\cdot(U_M - U_L) \tag{13}$$

where rand(0,1) is uniformly distributed and the solution of parameter estimation is feasible because they are initialized within the feasible range and we have to find the optimal one.

Step 2. According to (11) evaluate the fitness of each individual in the population.

Step 3. Create new population by:

(1) Mutation: For the given parameter vector U_i^k, randomly choose three different vectors (U_{r1}^k, U_{r2}^k, U_{r3}^k) in the range [1,NP]. A trial vector V_i^k is created by adding the third vector to the difference between the two vectors and is expressed as [34]:

$$V_i^k = U_{r1}^k + F\left(U_{r2}^k - U_{r3}^k\right) \tag{14}$$

where F is the mutation scaling factor having range (0,1).

(2) Crossover: The trial vector V_i^{k+1} and the target vector U_i^k are mixed to yield a new vector as [34]:

$$Y_i^k = \left[Y_{1i}^k, Y_{2i}^k, \ldots, Y_{ji}^k, \ldots, Y_{Qi}^k\right] \tag{15}$$

In this work, binomial crossover strategy [35] is used and it can be expressed as:

$$Y_{j,i}^k = \begin{cases} V_{j,i}^k, & if\left(rand_{i,j}(0,1) \le RC\right)\ or\ j = j_{rand} \\ U_{j,i}^k, & otherwise \end{cases} \tag{16}$$

where RC is the rate of crossover within the range (0,1).

(3) Penalty function:

If $V_{j,i}^k < U_L,\ then\ \ V_{j,i}^k = U_L - rand(0,1)\cdot(U_H - U_L)$ else $V_{j,i}^k > U_L,\ \ then\ V_{j,i}^k = U_H - rand(0,1)\cdot(U_H - U_L)$ end if.

(4) Selection: For each $U_{j,i}$ and corresponding $Y_{j,i}$, the condition to select next generation vector, k = k+1 is:

$$U_i^{k+1} = \begin{cases} Y_i^k, & \text{if } J\left(Y_i^k\right) < J\left(U_i^k\right) \\ U_i^k, & \text{otherwise} \end{cases} \tag{17}$$

where J(U) is the objective function to be minimized. Thus, the new trial vector swaps its values with the target; if the objective function value is less otherwise the target is conserved in the population.

3.2. Adaptive DE algorithm

The vector for the single diode and double diode model can be represented by U = [R_{ser}, R_{sh}, I_{sh}, I_{sd}, m] and U = [R_{ser}, R_{sh}, I_{sh}, I_{sd1}, I_{sd2} m_1, m_2] respectively. The parameter setting in DE is crucial [36,37] and to overcome this drawback an adaptive DE algorithm needs to be introduced [38,39]. The control parameters such as population, mutation, and crossover rates are adaptively controlled and generated by the parameters successfully. The adaptation is described as follows:

(1) Population adaptation:

The population with the Q-dimensional vectors $U_i^k = [U_{1,i}^k, U_{2,i}^k, \ldots, U_{j,i}^k, \ldots, U_{Q,i}^k]$ is an individual at the kth generation, k = 1,2, …,NP. The sum of Euclidean distances between individuals of a population is expressed as [47]:

$$Q^k = \sum_{i_1=1}^{NP} \sum_{i_{2=1}}^{i_1-1} \sqrt{\sum_{j=1}^{D} \left(U_{1,i,j}^k - U_{2,i,j}^k\right)^2} \tag{18}$$

If the population diversity is poor, it has the optimum convergence. In the case of stagnation, the algorithm does not occur at optimum value. In this case, a flag (F_U) is introduced to manage such condition and it is expressed as:

$$F_U = \begin{cases} 1, & \text{if } \alpha_j^k \geq ML \\ 0, & \text{otherwise} \end{cases} \tag{19}$$

$$\alpha_j^k = \begin{cases} \alpha_j^{k-1} + 1, & \text{if } Q^k = Q^k - 1 \\ 0, & \text{otherwise} \end{cases} \tag{20}$$

F_u indicates the status of population diversity. ML represents an integer whose value is set to NP; α_j^k represents the number of a generation that the distance between the individual population. If $\alpha_j^k = 1$ the new population $U_i^k + 1$, i = 1,2, …, NP can be generated as:

$$U_i^k + 1 = L_j^k + \left(H_j^k - L_j^k\right) \cdot randn_j^k, \quad j = 1, 2, \ldots, Q \tag{21}$$

where H_j^k = max(best$_j$, $U_{H,j}$); L_j^k = max(best$_j$, $U_{l,j}$); $U_{l,j}$, $U_{H,j}$ are the lower and upper bounds of the jth dimension of individuals respectively; $randn_j^k$ is a random number with the normal distribution.

(2) Mutation factor adaptation: The adaptation of mutation factor employs the approach of [47]. In order to maintain the population diversity, the mutation factor F_i is independently calculated for each vector as [47]:

$$F_i = \mathrm{rands}_i\left(P_F^k, 0.1\right) \tag{22}$$

$\mathrm{rands}_i(P_F^k, 0.1)$ is a random number generated with scale parameter 0.1 and location parameter P_F^k based on Cauchy distribution. The truncation is done if $F_i > 1.0$ or regeneration is performed if $F_i \leq 0$. The location parameter P_F is updated as:

$$P_F = (1 - s_i) \cdot P_F + s \cdot \mathrm{mean}_A(O_F) \tag{23}$$

where O_F is the set of all successful mutation factor Fi, at k generation; and mean$_A$(.) is the Lehmer mean and is expressed as:

$$\mathrm{mean}_A(O_F) = \frac{\sum_{i=1}^{|O_F|} F_i^2}{\sum_{i=1}^{|O_F|} F_i} \tag{24}$$

(3) Crossover rate adaptation: The crossover rate RC_i is independently calculated for each vector as [47]:

$$RC_i = randn_i\left(P_{RC}^k, 0.1\right) \tag{25}$$

where P_{RC}^k is the mean value to generate RC_i. It is updated as:

$$P_{RC} = (1 - s) \cdot P_{RC} + B \cdot mean_A(S_{RC}) \tag{26}$$

where B is a constant in the range (0,1); S_{RC} is the set of successful rate of RC_i and mean$_A$(.) is the usual arithmetic mean operation.

3.3. Importance of bypass and blocking diodes

A bypass diode (D_b) is connected in parallel with each panel where the panels are connected in series as shown in Fig. 4. In the normal mode of operation, this diode is reverse biased. When a cell gets damaged, it acts as a load instead of a generator. In this case, D_b maximizes the efficiency to allow the current through it from other cells present in the module. In order to minimize the power loss and maximize the efficiency, the bypass diode needs to have low forward voltage and low leakage current respectively. Moreover, the bypass diode has the capability to withstand power surges and high temperatures.

In addition, a blocking diode (D_k) is connected in series with the storage system (battery) to the PV module to prevent a current going backwards. During the night the potential across the PV cell drops to zero and the D_k prevents the current from reaching the battery and thus, the loss can be avoided.

To analyze the shaded condition of PV module, series and parallel connected modules are considered and are shown in Fig. 5(a) and (b) respectively. Assume that module-I is fully illuminated and module-II is partly shaded. The photocurrent generated by the shaded cell of module-II is EI_{ph}, where E represents the ratio of

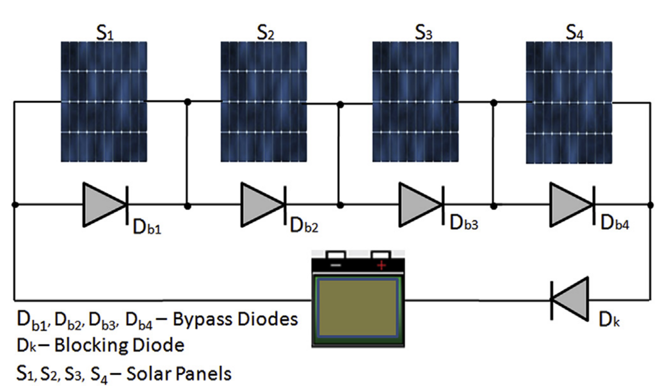

Fig. 4. Bypass and blocking diodes are connected with the PV module.

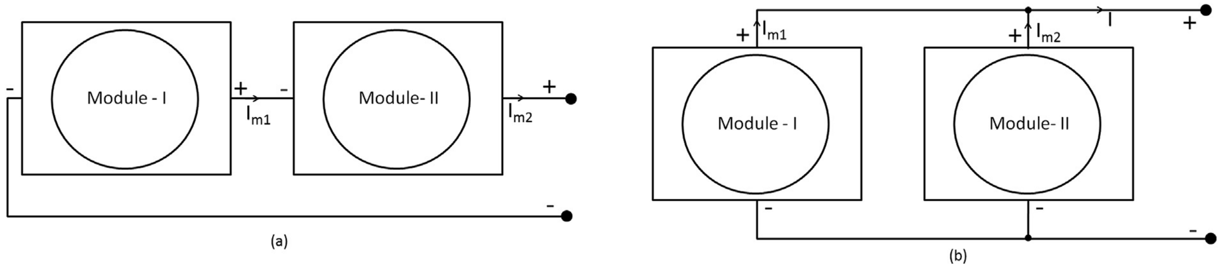

Fig. 5. Basic connections of solar modules (a) Serially connected (b) Parallel connected.

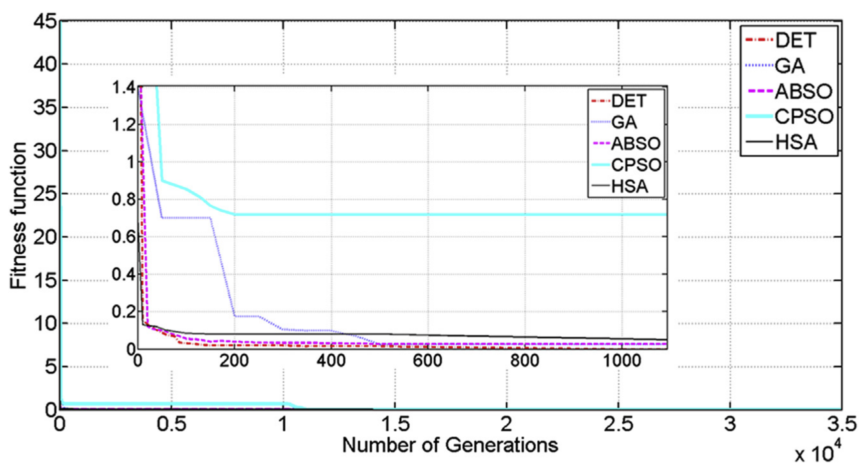

Fig. 6. Convergence characteristics of DET during parameter extraction for single diode model.

photocurrent generated by the shaded cell to fully illuminated cell. The value of E = 0 for shaded cell and E = 1 for the illuminated cell. The current in a solar cell under shaded illuminated condition can be expressed as:

$$I_s = EI_{ph} - I_{sd}\left[\exp\left(\frac{q(V_t + R_{ser}I_t)}{mkT_c}\right) - 1\right] - \left(\frac{V_t + R_{ser}I_t}{R_{sh}}\right), \quad \text{for shaded E} = 0 \tag{27}$$

In the same way, the current in a solar cell under illuminated condition can be expressed as:

$$I_i = I_{ph} - I_{sd}\left[\exp\left(\frac{q(V_t + R_{ser}I_t)}{mkT_c}\right) - 1\right] - \left(\frac{V_t + R_{ser}I_t}{R_{sh}}\right) \tag{28}$$

The illuminated and shaded cells are connected in series (refer Fig. 5(a)), with the same current $I_s = I_{m2}$, and the exponential term becomes zero under shaded condition. Therefore (27) can be simplified as:

$$I_{mo2} = EI_{ph} - I_{sd} - \left(\frac{V_s + R_{ser}I_t}{R_{sh}}\right) \tag{29}$$

Rearranging (29), voltage across the shaded cells V_s can be obtained as:

$$V_s = \left(EI_{ph} - I_{sd}\right)R_{sh} - R_{ser}I_t \tag{30}$$

From (29) and (30), the power dissipated by the shaded cell can be expressed as:

$$P_s = I_{m2}\left[\left(EI_{ph} - I_{sd}\right)R_{sh} - R_{ser}I_t\right] \tag{31}$$

The total voltage of serially connected array is the sum of individual module, which is fully illuminated and the shaded cells in the same module can be expressed as:

$$V_m = \sum_{j=1}^{a} V_{ij} + \sum_{j=1}^{b} V_{sj} \tag{32}$$

In case parallel connected modules

$$I = I_{m1} + I_{m2} = I_{m1} + EI_{ph} - I_{sd} - \left(\frac{V_s + R_{ser}I_{m2}}{R_{sh}}\right) \tag{33}$$

4. Simulation and experimental results

In this section, the parameters of DET have been studied by using measured data. The measured voltage, current data of solar

Table 1
Comparison of various parameter extraction methods for single diode model.

Items	CPSO	GA	HSA	ABSO	DET
I_{ph} (A)	0.761	0.762	0.761	0.761	0.751
I_{sd} (A)	0.400	0.809	0.305	0.307	0.315
m	1.504	1.575	1.475	1.477	1.487
R_{ser} (Ω)	0.035	0.029	0.037	0.038	0.036
R_{sh} (Ω)	59.013	42.373	53.595	52.301	54.532
RMSE	0.0015	0.0191	9.950×10^{-4}	9.9124×10^{-4}	9.3×10^{-4}
Time (s)	0.25	0.26	0.27	0.26	0.24

Table 2
Optimal values of IAE and RE extracted by HSA, ABSO and DET for single diode model.

Meas.	Vm (V)	I_{me} (A)	HSA algorithm			ABSO algorithm			DET algorithm		
			I_{es} (A)	IAE	RE	I_{es} (A)	IAE	RE	I_{es} (A)	IAE	RE
1	−0.2057	0.7640	0.7645	0.0003	−0.0005	0.7643	0.0003	−0.0003	0.7641	0.0001	−0.0001
2	−0.1291	0.7620	0.7628	0.0009	−0.0010	0.7627	0.0007	−0.0009	0.7625	0.0005	−0.0006
3	−0.0588	0.7605	0.7614	0.0013	−0.0011	0.7613	0.0008	−0.0010	0.7612	0.0007	−0.0009
4	0.0057	0.7605	0.7602	0.0000	0.0003	0.7601	0.0004	0.0005	0.7602	0.0003	0.0003
5	0.0646	0.7600	0.7591	0.0009	0.0011	0.7590	0.0010	0.0013	0.7591	0.0009	0.0011
6	0.1185	0.7590	0.7577	0.0007	0.0016	0.7579	0.0011	0.0014	0.7580	0.0001	0.0001
7	0.1678	0.7570	0.7570	0.0007	−0.0000	0.7570	0.0000	0.0000	0.7570	0.0000	−0.0009
8	0.2132	0.7570	0.7561	0.0008	0.0011	0.7560	0.0010	0.0013	0.7561	0.0009	0.0011
9	0.2545	0.7555	0.7548	0.0007	0.0009	0.7549	0.0006	0.0007	0.7550	0.0005	0.0006
10	0.2924	0.7540	0.7533	0.0007	0.0009	0.7535	0.0005	0.0006	0.7536	0.0004	0.0005
11	0.3269	0.7505	0.7513	0.0008	−0.0010	0.7512	0.0007	−0.0009	0.7510	0.0005	−0.0006
12	0.3585	0.7465	0.7473	0.0008	−0.0010	0.7472	0.0007	−0.0009	0.7470	0.0005	−0.0006
13	0.3873	0.7385	0.7406	0.0021	−0.0028	0.7405	0.0020	−0.0027	0.7403	0.0018	−0.0024
14	0.4137	0.7280	0.7272	0.0008	0.0010	0.7274	0.0006	0.0008	0.7274	0.0006	0.0008
15	0.4373	0.7065	0.7071	0.0006	−0.0008	0.7070	0.0005	−0.0007	0.7068	0.0003	−0.0004
16	0.4590	0.6755	0.6751	0.0004	0.0005	0.6752	0.0003	0.0004	0.6754	0.0001	0.0001
17	0.4784	0.6320	0.6308	0.0012	0.0018	0.6309	0.0011	0.0017	0.6308	0.0012	0.0018
18	0.4960	0.5730	0.5723	0.0007	0.0012	0.5722	0.0008	0.0013	0.5723	0.0007	0.0012
19	0.5119	0.4990	0.4996	0.0006	−0.0012	0.4996	0.0006	−0.0012	0.4994	0.0004	−0.0008
20	0.5265	0.4130	0.4136	0.0006	−0.0014	0.4135	0.0005	−0.0012	0.4133	0.0003	−0.0007
21	0.5398	0.3165	0.3172	0.0007	−0.0022	0.3171	0.0006	−0.0018	0.3169	0.0004	−0.0012
22	0.5521	0.2120	0.2118	0.0002	0.0009	0.2121	0.0001	−0.0004	0.2120	0.0000	−0.0000
23	0.5633	0.1035	0.1024	0.0011	0.0115	0.1026	0.0009	0.0086	0.1027	0.0008	0.0077
24	0.5736	−0.0100	−0.0095	0.0005	0.0500	−0.0096	0.0004	0.0400	−0.0095	0.0005	0.0500
25	0.5833	−0.1320	−0.1244	0.0076	0.0575	−0.1245	0.0075	0.0568	−0.1247	0.0073	0.0553
26	0.5900	−0.2100	−0.2092	0.0008	0.0038	−0.2093	0.0007	0.0033	−0.2095	0.0005	0.0023

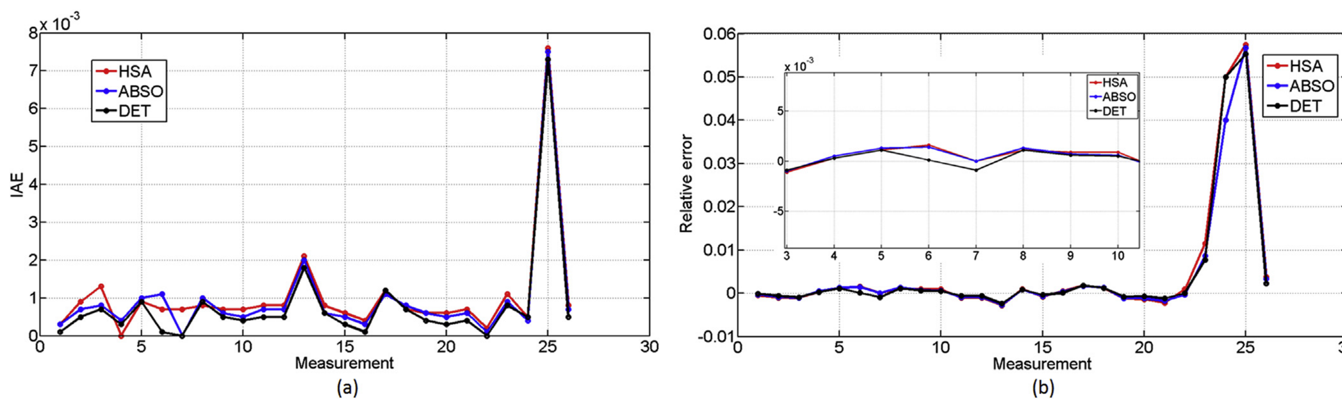

Fig. 7. Optimal values extracted by ABSO, HSA and DET for single diode mode (a) Individual absolute error (b) Relative error.

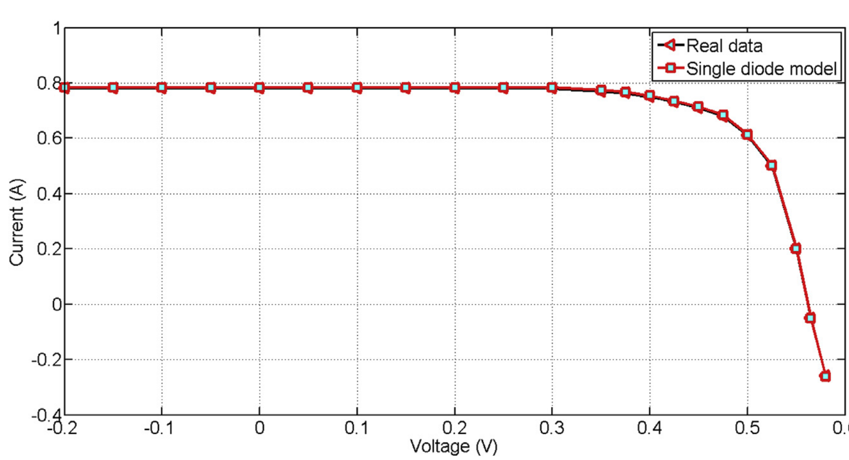

Fig. 8. Comparison results of single diode model with the real data.

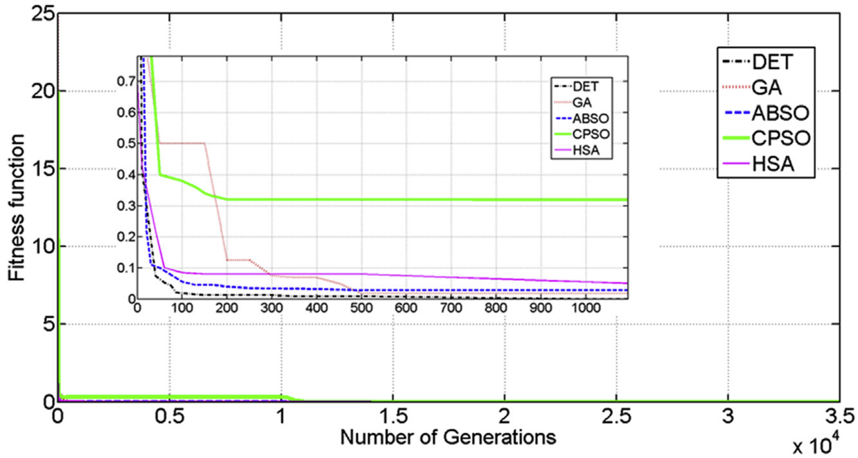

Fig. 9. Convergence characteristics of DET during parameter extraction for double diode model.

Table 3
Comparison of various parameter extraction methods for double diode model.

Items	HSA	ABSO	SA	PS	DET
I_{ph} (A)	0.76176	0.76067	0.7620	0.7608	0.76098
I_{sd1} (μA)	0.12546	0.26713	0.4674	0.9793	0.33267
I_{sd2} (μA)	0.25473	0.38193	0.0110	0.00013	0.0647
m_{i1}	1.49436	1.46521	1.4948	1.6298	1.48735
m_{i2}	1.49986	1.98146	2.0001	1.1936	1.7956
R_{ser} (Ω)	0.03543	0.03648	0.0356	0.0321	0.03685
R_{sh} (Ω)	46.8264	54.6274	43.2945	82.036	54.5321
RMSE	0.001264	0.000983	0.017035	0.015482	0.000924
Time(s)	0.24	0.25	0.25	0.26	0.22

cell, and PV modules has been used in this simulation. The prototype has a 5.8 cm diameter silicon solar cell, and the voltage and the current are measured under one sun at 30 °C (1000 W/m^2). On the other hand, the prototype of the PV modules have 36 polycrystalline silicon and are connected in series, and the voltage and current are measured under one sun at 33 °C (1000 W/m^2). Various parameters of DET used in this simulation as follows: the population size NP = 150, the maximum number of generation k_{max} = 500, Length of individual L_i = 3, DE-step size S = 0.5, merging generation rate P_m = 0.5, crossover probability constant C_r = 0.5, and the termination criteria $T_c = 1 \times e^{-6}$.

4.1. Single diode model

The ability of DET to extract various parameters of single diode model is carried out. Here, 26 pairs of V-I values, which are same as in Ref. [42], are used as the measured data. The convergence process of DET under parameter extraction is shown in Fig. 6. The extracted optimal parameters such as I_{ph}, I_{sd}, m, R_{ser}, R_{sh} and RMSE for single diode model are presented in Table 1.

The proposed DET method is compared with other parameters

Table 4
Optimal values of IAE and RE extracted by HSA, ABSO and DET for double diode model.

Meas.	Vm (V)	I_{me} (A)	HSA algorithm			ABSO algorithm			DET algorithm		
			I_{es} (A)	IAE	RE	I_{es} (A)	IAE	RE	I_{es} (A)	IAE	RE
1	−0.2057	0.7640	0.7640	0.0000	−0.0000	0.7640	0.0000	0.0000	0.7640	0.0000	0.0000
2	−0.1291	0.7620	0.7627	0.0007	−0.0009	0.7626	0.0006	−0.0007	0.7626	0.0006	−0.0007
3	−0.0588	0.7605	0.7613	0.0008	−0.0010	0.7613	0.0008	−0.0010	0.7613	0.0008	−0.0010
4	0.0057	0.7605	0.7601	0.0004	0.0006	0.7601	0.0004	0.0005	0.7602	0.0003	0.0003
5	0.0646	0.7600	0.7590	0.0010	0.0013	0.7590	0.0010	0.0013	0.7591	0.0009	0.0011
6	0.1185	0.7590	0.7579	0.0011	0.0013	0.7580	0.0010	0.0013	0.7580	0.0010	0.0013
7	0.1678	0.7570	0.7571	0.0001	−0.0001	0.7571	0.0001	−0.0001	0.7570	0.0000	0.0000
8	0.2132	0.7570	0.7561	0.0009	0.0011	0.7561	0.0009	0.0011	0.7562	0.0008	0.0010
9	0.2545	0.7555	0.7550	0.0005	0.0006	0.7551	0.0004	0.0005	0.7551	0.0004	0.0005
10	0.2924	0.7540	0.7536	0.0004	0.0005	0.7536	0.0004	0.0005	0.7537	0.0003	0.0003
11	0.3269	0.7505	0.7514	0.0009	−0.0011	0.7513	0.0008	−0.0010	0.7514	0.0009	−0.0011
12	0.3585	0.7465	0.7473	0.0008	−0.0010	0.7473	0.0008	−0.0010	0.7472	0.0007	−0.0009
13	0.3873	0.7385	0.7401	0.0016	−0.0021	0.7400	0.0015	−0.0020	0.7400	0.0015	−0.0020
14	0.4137	0.7280	0.7273	0.0007	0.0009	0.7273	0.0007	0.0009	0.7272	0.0008	0.0010
15	0.4373	0.7065	0.7069	0.0004	−0.0005	0.7068	0.0003	−0.0004	0.7068	0.0003	−0.0004
16	0.4590	0.6755	0.6753	0.0002	0.0002	0.6753	0.0002	0.0002	0.6754	0.0001	0.0000
17	0.4784	0.6320	0.6309	0.0011	0.0017	0.6309	0.0011	0.0017	0.6310	0.0010	0.0015
18	0.4960	0.5730	0.5721	0.0009	0.0015	0.5721	0.0009	0.0015	0.5721	0.0009	0.0015
19	0.5119	0.4990	0.4996	0.0006	−0.0012	0.4996	0.0006	−0.0012	0.4995	0.0005	−0.0010
20	0.5265	0.4130	0.4134	0.0004	−0.0009	0.4133	0.0003	−0.0007	0.4132	0.0002	−0.0004
21	0.5398	0.3165	0.3172	0.0007	−0.0022	0.3172	0.0007	−0.0022	0.3171	0.0006	−0.0018
22	0.5521	0.2120	0.2121	0.0001	−0.0004	0.2120	0.0000	−0.0000	0.2120	0.0000	−0.0000
23	0.5633	0.1035	0.1027	0.0008	0.0077	0.1027	0.0008	0.0077	0.1026	0.0009	0.0086
24	0.5736	−0.0100	−0.0080	0.0020	0.2000	−0.0080	0.0020	0.2000	−0.0090	0.0010	0.1000
25	0.5833	−0.1320	−0.1282	0.0038	0.0287	−0.1283	0.0037	0.0280	−0.1285	0.0035	0.0265
26	0.5900	−0.2100	−0.2090	0.0010	0.0047	−0.2090	0.0020	0.0095	−0.2091	0.0009	0.0042

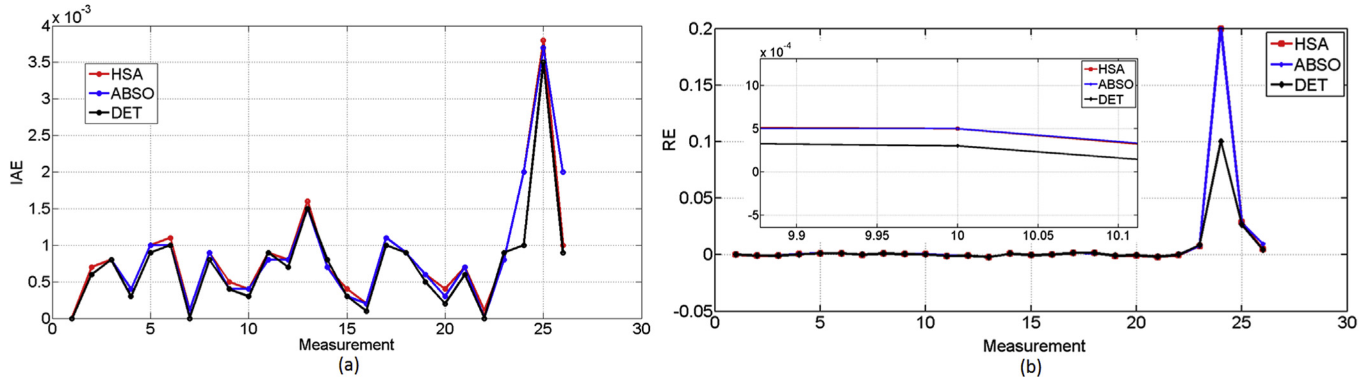

Fig. 10. Optimal values extracted by ABSO, HSA and DET for double diode model (a) Individual Absolute error (b) Relative error.

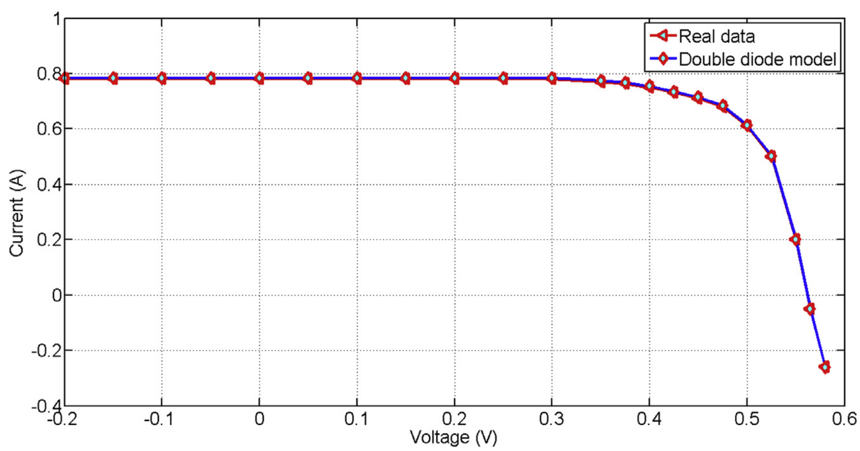

Fig. 11. Comparison results of double diode model with the real data.

Table 5
Comparison of various parameter extraction methods for the PV module.

Items	CPSO	ABSO	OIS	1DAB	PS	SA	HSA	DET
I_{ph} (A)	1.0254	1.03166	1.03674	1.04276	1.0324	1.0334	1.0635	1.03045
I_{sd} (A)	3.0743	3.3731	3.1946	3.4265	3.1859	3.6387	3.7245	3.31089
m_i	52.237	48.5832	49.0435	49.2843	48.2467	48.7934	48.436	48.4379
R_{ser} (Ω)	1.0735	1.20134	1.32897	1.73762	1.304	1.2042	1.1046	1.1063
R_{sh} (Ω)	1850.100	852.463	1184.58	948.845	742.2156	843.5233	824.646	815.647
RMSE	0.003521	0.00227	0.004783	0.00536	0.0127	0.00285	0.00365	0.002131
Time (s)	0.29	0.31	0.32	0.31	0.32	0.33	0.29	0.27

extraction methods such as chaos particle swarm optimization (CPSO) [23], genetic algorithm (GA) [41], harmony search algorithm (HSA) [42], and artificial bee swarm optimization (ABSO) [42]. Various parameters and RMSE value of these extraction methods are listed in Table 1. From Table 1, it is indicated that the DET provides the lowest RMSE compared to other techniques. Table 1 also indicates that DET has the lowest RMSE while the ABSO has the second lowest RMSE among other methods. The RMSE values of HSA and ABSO are very close to DET, therefore, these techniques can be used for a detailed study. The relative error (RE) and individual absolute error (IAE) are used to show the performance of parameter extraction methods [40] and it can be defined as:

$$IAE = |I_{me} - I_{es}| \tag{34}$$

$$RE = \frac{|I_{me} - I_{es}|}{I_{me}} \tag{35}$$

The optimal values of each measurement of IAE and RE for ABSO, HSA, and DET have been summarized in Table 2. The value of IAE and RE have been calculated for each optimal values extracted by ABSO, HSA, and DET. The comparison between ABSO, HSA and the proposed method with the optimal value of IAE and RE for each measurement is illustrated in Fig. 7. From Fig. 7 one can easily understand that the DET method has better performance than ABSO and HSA techniques. In order to study the quality of optimal values extracted by DET, various parameters such as R_{ser}, R_{sh}, I_{ph}, I_{sd} and m are substituted into (2), and then the I-V characteristics of single diode model are found. Fig. 8 illustrates the I-V characteristics of optimal values extracted by DET along with the measured data.

Table 6
Optimal values of IAE extracted by CPSO, ABSO, PS, SA, OIS, DAB and DET for the PV module.

Item	Vm(V)	I_{me} (A)	CPSO	ABSO	OIS	DAB	PS	SA	DET
1	0.1243	1.0401	0.00135	0.00134	0.00140	0.00227	0.00213	0.00009	0.00121
2	1.8090	1.0380	0.00194	0.00168	0.00317	0.00359	0.00345	0.00072	0.00154
3	3.3502	1.0329	0.00058	0.00049	0.00136	0.00282	0.00168	0.00148	0.00034
4	4.7603	1.0278	0.00269	0.00242	0.00098	0.00157	0.00138	0.00354	0.00229
5	6.0512	1.0223	0.00471	0.00446	0.00213	0.00032	0.00064	0.00532	0.00418
6	7.2343	1.0183	0.00463	0.00427	0.00354	0.00116	0.00129	0.00567	0.00389
7	8.3166	1.0136	0.00245	0.00214	0.00095	0.00389	0.00465	0.00287	0.00203
8	9.3065	1.0098	0.00043	0.00024	0.00254	0.00679	0.00687	0.00089	0.00018
9	10.2142	1.0042	0.00327	0.00287	0.00685	0.01047	0.01058	0.00276	0.00261
10	11.0421	0.9920	0.00385	0.00354	0.00734	0.01179	0.01137	0.00389	0.00342
11	11.8001	0.9710	0.00379	0.00365	0.00690	0.01197	0.01176	0.00427	0.00348
12	12.4902	0.9411	0.00283	0.00256	0.00523	0.01214	0.00864	0.00327	0.00232
13	13.1893	0.8927	0.00019	0.00010	0.00241	0.00814	0.00811	0.00103	0.00007
14	13.6145	0.8205	0.00042	0.00035	0.00212	0.00785	0.00421	0.00148	0.00021
15	14.2146	0.7316	0.00162	0.00160	0.00038	0.00513	0.00325	0.00045	0.00145
16	14.6821	0.6298	0.00206	0.00219	0.00157	0.00367	0.00302	0.00136	0.00197
17	15.1246	0.5184	0.00140	0.00130	0.00110	0.00312	0.00175	0.00046	0.00112
18	15.5272	0.4134	0.00116	0.00101	0.00046	0.00184	0.00243	0.00098	0.00094
19	15.8893	0.3046	0.00034	0.00021	0.00175	0.00228	0.00269	0.00079	0.00013
20	16.2265	0.2013	0.00089	0.00064	0.00489	0.00298	0.00594	0.00195	0.00042
21	16.2613	0.0934	0.00220	0.00198	0.00068	0.00516	0.00073	0.00593	0.00170
22	16.2834	−0.0010	0.00025	0.00019	0.00016	0.00084	0.00138	0.00069	0.00013
23	17.0509	−0.1226	0.00009	0.00002	0.00037	0.00229	0.00376	0.00008	0.00003
24	17.2734	−0.2416	0.00057	0.00043	0.00009	0.00376	0.00435	0.00003	0.00031
25	17.4875	−0.3698	0.00093	0.00082	0.00036	0.00684	0.00653	0.00350	0.00064
Total IAE			0.04464	0.04050	0.05873	0.12268	0.10395	0.0535	0.03661

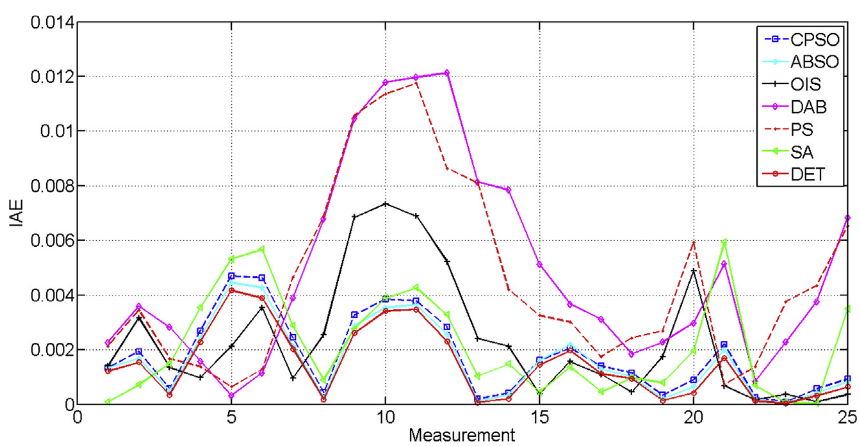

Fig. 12. Optimal values of IAE extracted by CPSO, ABSO, PS, SA, OIS, DAB and DET for the PV module.

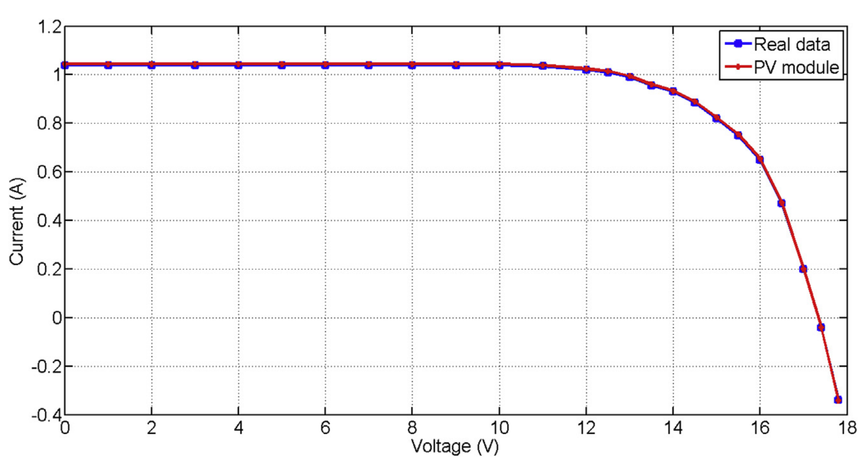

Fig. 13. Comparison results of PV module with the real data.

Table 7
Experimental results of the proposed parameter extraction method.

Model	Type	Current (A)	Resistance (Ω)	Ideality factor	RMSE
Single diode model	Mono-crystalline (SM55)	$I_{ph} = 4.92$ $I_{sd} = 3.36 \times 10^{-10}$	$R_{ser} = 0.63$ $R_{sh} = 351.75$	m = 1.264	0.026
	Multi-crystalline (KC 200GT)	$I_{ph} = 7.01$ $I_{sd} = 4.28 \times 10^{-10}$	$R_{ser} = 0.34$ $R_{sh} = 162.24$	m = 1.02	0.023
Double diode model	Mono-crystalline (SM55)	$I_{ph} = 5.02$ $I_{sd1} = 3.62 \times 10^{-10}$ $I_{sd2} = 3.94 \times 10^{-10}$	$R_{ser} = 0.61$ $R_{sh} = 210.19$	$m_1 = 1.01$ $m_2 = 1.29$	0.022
	Multi-crystalline (KC 200GT)	$I_{ph} = 6.934$ $I_{sd1} = 4.25 \times 10^{-10}$ $I_{sd2} = 4.28 \times 10^{-10}$	$R_{ser} = 0.34$ $R_{sh} = 160.64$	$m_1 = 1.04$ $m_2 = 1.36$	0.021
PV module	Mono-crystalline (SM55)	$I_{ph} = 4.89$ $I_{sd} = 3.36 \times 10^{-10}$	$R_{ser} = 0.72$ $R_{sh} = 276.46$	m = 1.17	0.026
	Multi-crystalline (KC 200GT)	$I_{ph} = 4.80$ $I_{sd1} = 4.28 \times 10^{-10}$	$R_{ser} = 0.92$ $R_{sh} = 156.6$	m = 1.09	0.028

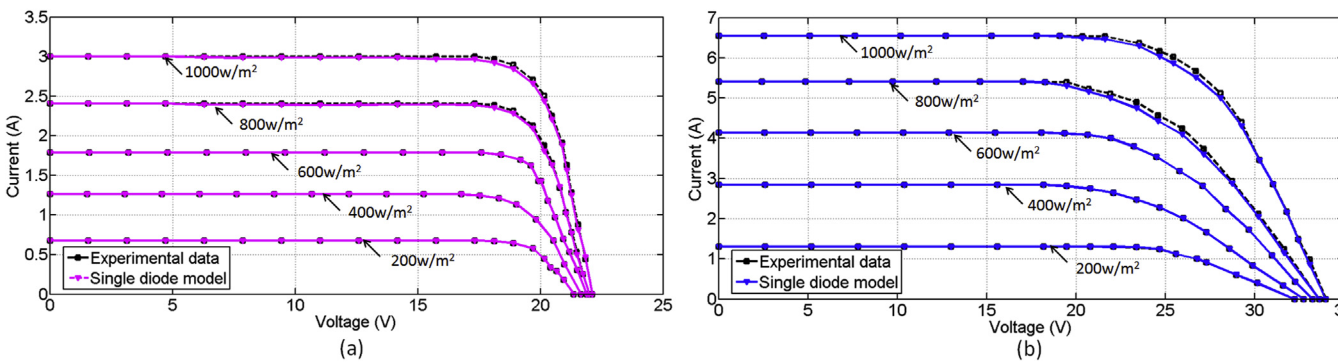

Fig. 14. V-I curve of the experimental data and the extracted single diode model (a) mono-crystalline (b) multi-crystalline.

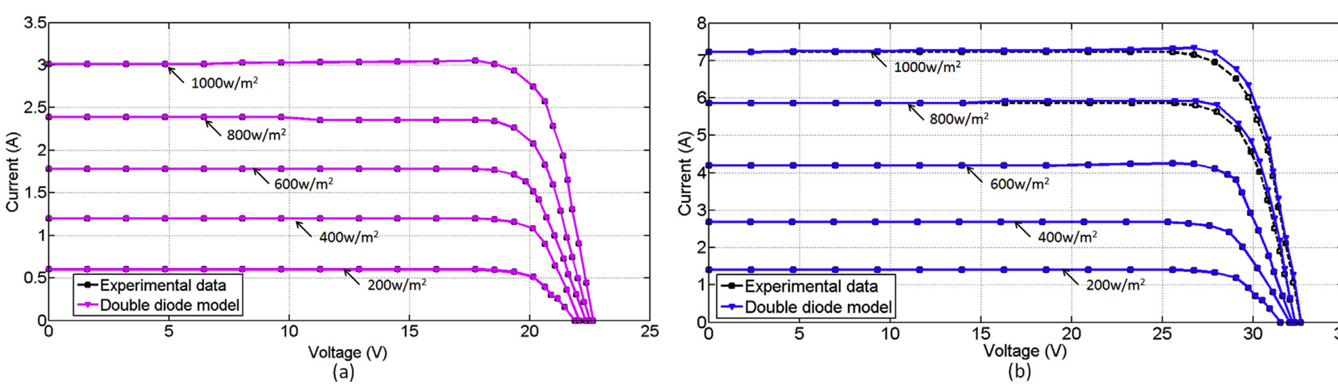

Fig. 15. V-I curve of the experimental data and the extracted double diode model (a) mono-crystalline (b) multi-crystalline.

4.2. Double diode model

The ability of DET to extract different parameters of double diode model is demonstrated. The 26 pairs' real value is used in a single diode model and is also considered in this model. The convergence process of DET under parameter extraction is shown in Fig. 9. The extracted optimal parameters such as I_{ph}, I_{sd1}, I_{sd2}, m_1, m_2, R_{ser}, R_{sh}, and RMSE for double diode model are listed in Table 3.

The proposed DET method is compared with other parameter extraction methods such as harmony search algorithm (HSA) [42], artificial bee swarm optimization (ABSO) [42], simulated annealing (SA) [43] and pattern search (PS) [41]. Various parameters and RMSE value of these extraction methods are listed in Table 3. Table 3 indicates that the DET provides the lowest RMSE compared to other parameter extraction techniques. Table 3 points out that DET has lowest RMSE and ABSO and HSA has second and third lowest RMSE respectively among the methods which are considered for comparison. The RMSE values of HSA and ABSO are very close to DET, so these two techniques were studied in detail. The optimal values of IAE and RE of each measurement extracted by the HSA, ABSO and DET are listed in Table 4. The comparison between ABSO, HSA and the proposed method with the optimal value of IAE and RE for each measurement is illustrated in Fig. 10. From Fig. 10 it is indicated that the DET method performs better than ABSO and HSA techniques.

In order to study the quality of optimal values extracted by DET, various parameters such as R_{ser}, R_{sh}, I_{ph}, I_{sd1}, I_{sd2}, m_1, and m_2 are substituted into (6), then the I-V characteristics of double diode

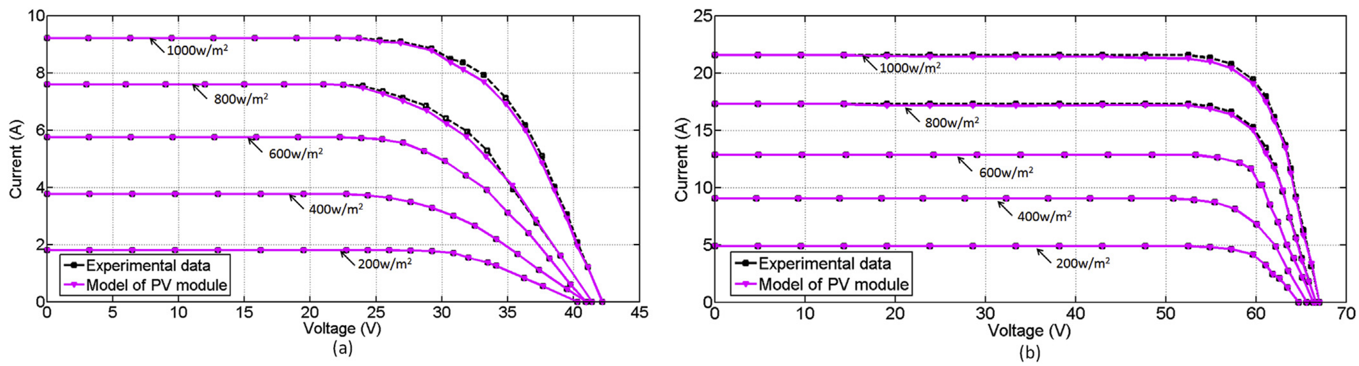

Fig. 16. V-I curve of the experimental data and the extracted model of PV module (a) mono-crystalline (b) multi-crystalline.

models are found. Fig. 11 illustrates the I-V characteristics of optimal values extracted by DET along with the real data. From the results, it is observable that the double diode model is the best choice for the measured data.

4.3. Model of PV modules

The prototype of PV module has 6 solar panels, two are connected in series and three PV panels are connected in parallel and the measured voltage and current are taken under one sun at 33 °C (1000 W/m^2). The real values of voltage and current of PV modules are the same as [44]. The optimal parameter values and the RMSE of proposed method are listed in Table 5. The proposed DET method is compared with other parameter extraction techniques such as CPSO, ABSO, PS, SA, the I-V characteristics of organic and inorganic solar cells studied by Chegaar et al. (OIS) [45] and the solar cell parameters evaluation studied by Bouzidi et al. called (DAB) [46] is used from the dark experiment data. The comparison between DET and other parameter extraction methods are listed in Table 5. It proves that the DET has the lowest RMSE compared to other parameter extraction techniques such as CPSO, ABSO, PS, SA, OIS, and DAB. Since DET has the lowest RMSE, the performance of DET is optimal and is suitable for parameter extraction in a solar module.

The optimal value of IAE for each measurement using DET and other parameter extraction techniques such as CPSO, ABSO, PS, SA, OIS, and DAB are listed in Table 6. The comparison between CPSO, ABSO, PS, SA, OIS, DAB, and the proposed method with the optimal value of IAE for each measurement is illustrated in Fig. 12. From Fig. 12 it is indicated that the DET method have better performances than other parameters extraction methods such as CPSO, ABSO, PS, SA, OIS, and DAB. The total IAE values for each measurement is also calculated and listed in Table 6. The total IAE value of Table 6 points out that the DET has the lowest total IAE compared to other methods for the PV module. From Table 6 and Fig. 12 it is indicated that DET outperforms CPSO, ABSO, PS, SA, OIS, and DAB for this parameter extraction problem.

In order to study the quality of optimal values extracted by DET, various parameters such as R_{ser}, R_{sh}, I_{ph}, I_{sd} and m are substituted into (7) and then determined by the I-V characteristics of PV module. Fig. 13 illustrates the I-V characteristics of optimal values extracted by DET along with the real data. From the results, it is observed that the values extracted by DET in the PV module fit the real data very well.

4.4. Experimental test

The parameter extraction methods used for solar cell models such as single diode model, double diode model, and PV module have been tested with experiments. For all the models both the monocrystalline type solar module (SM 55) and multi-crystalline type solar module (KC 200GT) are used for testing and the mono and multi-crystalline array (2 × 3) has been used for PV modules. For easy computation, the variation present in the temperature is not included here. The experiment is conducted for five different irradiance levels such as 200 W/m^2, 400 W/m^2, 600 W/m^2, 800 W/m^2 and 1000 W/m^2 and the data is measured simultaneously for each level. The experimental data extracted from the three different models are listed in Table 7. Table 7 indicates that the value of RMSE is very low for the three models using the proposed technique. Figs. 14–16 shows the voltage-current characteristic curve obtained by DET method for the three models using different irradiance levels. Fig. 14 shows the I-V characteristics of single diode model for mono and multi-crystalline solar modules. From Fig. 14 it is understandable that the extracted values almost match the experimental data. In particular, the values are well suited for low irradiance level and slight variation is exhibited in higher irradiance level in the proposed technique. Accurate extraction of parameters is very crucial at low irradiance exactly when the module meets certain mismatching conditions. Fig. 15 shows the I-V characteristics of double diode model for mono and multi-crystalline solar modules. From Fig. 15 it is indicated that the extracted values exactly match with the experimental data for multi-crystalline solar modules. In particular, slight variation is exhibited only in higher irradiance level of mono-crystalline solar modules. Fig. 16 indicates the V-I characteristics of PV module for both the mono-crystalline and multi-crystalline solar modules. From Fig. 16, it is indicated that the extracted values match the low irradiance of mono-crystalline and it exactly matches all the irradiance of multi-crystalline solar modules. The experimental results of different solar cell models are listed in Table 7 and Figs. 14–16. The performance of the proposed parameter extraction method is verified with accuracy. From this, the proposed DET technique provides optimal performance in parameter extraction of PV models.

The bypass diodes are usually connected on each sub-string to eliminate the hot-spot phenomenon and increase the reliability. The MATLAB Simscape libraries contain the basic components (PV cells, bypass diodes, etc.) and the PV array can be easily modeled

Table 8
Electrical characteristics of two different PV modules.

Designation	KC 200GT	SM 55
Maximum power (P_{max})	200 W	55W
Voltage at P_{max} (V_{PPM})	26.3 V	17.4 V
Current at P_{max} (I_{PPM})	7.61 A	3.15 A
Open circuit voltage (V_{oc})	32.9 V	21.7 V
Short circuit current (I_{sc})	8.21 A	3.45 A
Number of cells	54	36

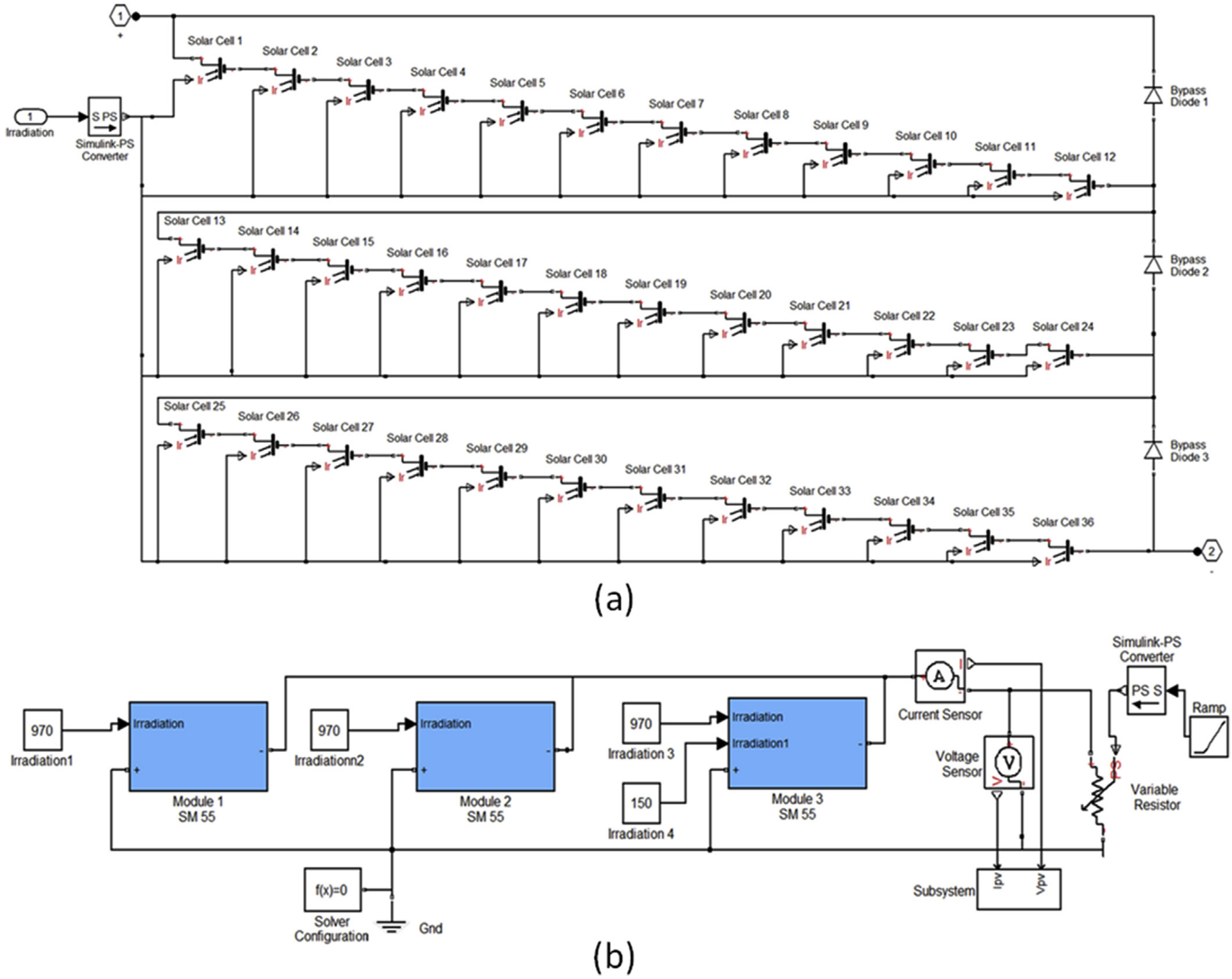

Fig. 17. Implementation using Simscape (a) the PV module "KC 200GT" with bypass diodes and (b) the PV array.

using [48]. The commercial PV module KC 200GT with 200 W is selected and the parameters are obtained from the data sheet. The electrical characteristics of two different modules are listed in Table 8.

The PV array can be created under partially shaded conditions (PSCs) in Matlab-based Simscape. Moreover, bypass diodes are added parallel to PV cells in order to avoid the localized power dissipation. The PV module KC 200GT with 32 multi-crystalline silicon solar cell is characterized by its electrical features which are listed in Table 8 and are modeled by Simscape as shown in Fig. 17. The PV array consists of three modules, which are connected parallel to non-uniform irradiance level. The PV modules (KC 200GT and SM 55) have been modeled with different electrical characteristics under two different shading patterns which are listed in Table 9. The two shading patterns have been carried out for the three series-connected module type KC 200GT with 200 W and three parallel connected module type SM 55 with 65 W. The effectiveness of the developed Simscape has been verified by the measured P-V characteristics. Fig. 18 shows that the simulated and experimental results of case 1 and 2 of KC 200GT. Fig 18(a) and (b) indicates that two power peaks have been obtained from case 1and three power peaks have been observed from case 2 respectively. The P-V characteristics of case I and 2 of SM 55 module is shown in Fig. 19(a) and (b) respectively. Under case 1, the shaded PV module of SM 55 receives an insolation level of 960 W/m^2 and the other two receive 140 W/m^2. While under case 2, the two shaded PV module of SM 55 receives an insolation level of 970 W/m^2 and the remaining one receives 150 W/m^2. It is indicated that two power peaks have been observed at 63 W and 12 W for case 1 and at 35 W and 34 W for case 2 respectively. From Figs. 18 and 19, it is indicated that an agreement has been observed between the measured and simulated P-V characteristics for all the shading conditions.

The performance criteria of different algorithms are described in

Table 9
Various shading pattern for two different solar modules.

Designation	KC 200GT	SM 55
Case 1	Module #1 = 140 W/m^2	Module #1 = 960 W/m^2
	Module #2 = 970 W/m^2	Module #2 = 140 W/m^2
	Module #3 = 970 W/m^2	Module #3 = 140 W/m^2
Case 2	Module #1 = 500 W/m^2	Module #1 = 970 W/m^2
	Module #2 = 930 W/m^2	Module #2 = 970 W/m^2
	Module #3 = 700 W/m^2	Module #3 = 150 W/m^2
Temperature (°C)	27.5	29

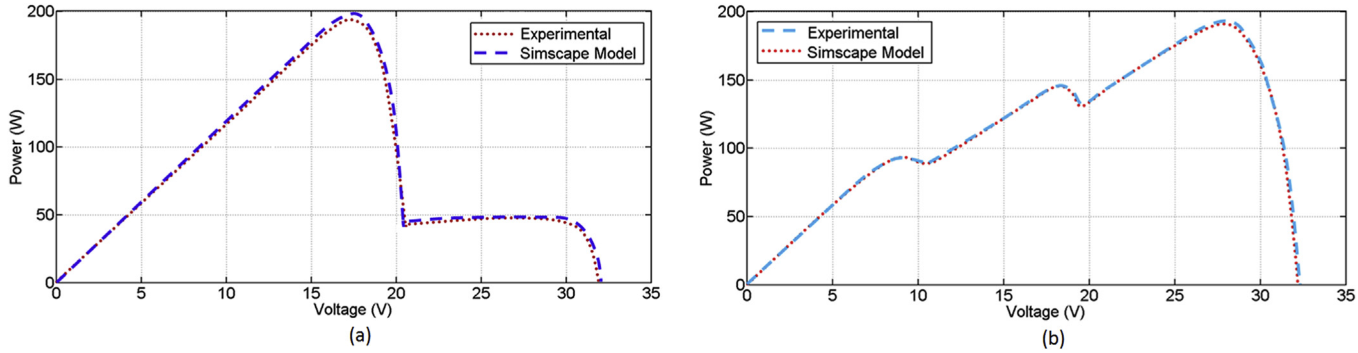

Fig. 18. P-V characteristics of module KC 200GT (a) case 1 and (b) case 2.

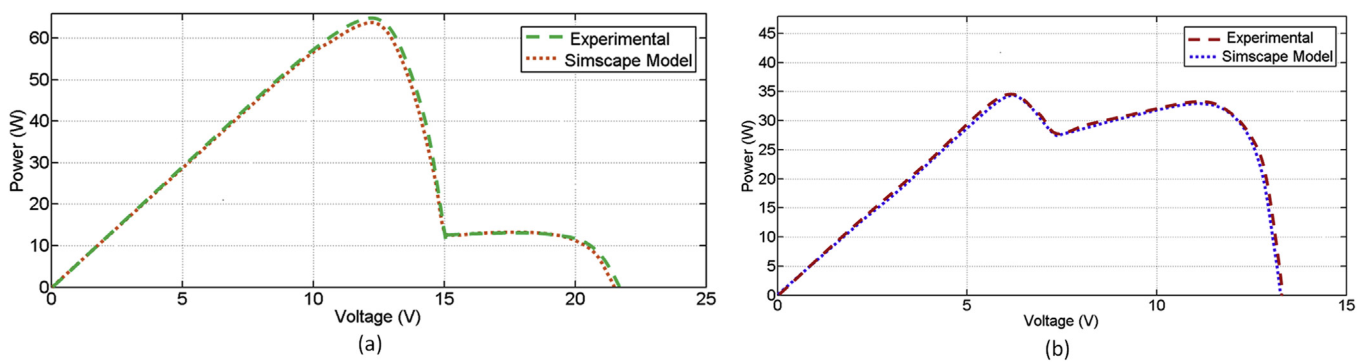

Fig. 19. P-V characteristics of module SM 55 (a) case 1 and (b) case 2.

Table 10
Comparison of different performance criteria of single diode model, double diode model and model of PV module.

Algorithm	Minimum	Median	Maximum	Mean	Std. Deviation	Success rate
RMSE Single diode model						
CPSO	9.52317×10^{-04}	1.02748×10^{-03}	2.63799×10^{-03}	1.46238×10^{-03}	1.734×10^{-04}	0.42
HSA	1.02317×10^{-03}	1.26836×10^{-03}	2.62627×10^{-03}	1.26474×10^{-03}	1.923×10^{-04}	0.24
ABSO	9.38217×10^{-04}	9.47238×10^{-04}	1.83628×10^{-03}	1.00373×10^{-03}	2.734×10^{-05}	0.53
SA	1.18251×10^{-03}	1.36452×10^{-03}	1.73626×10^{-03}	1.24628×10^{-03}	1.243×10^{-04}	0.42
DET	8.58297×10^{-04}	8.92648×10^{-04}	8.92366×10^{-04}	8.93617×10^{-04}	5.346×10^{-08}	0.94
RMSE Double diode model						
CPSO	9.42491×10^{-04}	1.18231×10^{-03}	3.17453×10^{-03}	1.61637×10^{-03}	2.283×10^{-04}	0.47
HSA	1.18436×10^{-03}	1.29624×10^{-03}	3.72401×10^{-03}	1.42381×10^{-03}	2.623×10^{-04}	0.32
ABSO	9.21278×10^{-04}	1.09925×10^{-03}	2.38120×10^{-03}	1.38252×10^{-03}	1.132×10^{-04}	0.61
SA	1.27157×10^{-03}	1.52422×10^{-03}	2.28451×10^{-03}	1.52638×10^{-03}	1.478×10^{-04}	0.58
DET	8.42473×10^{-04}	8.91346×10^{-04}	8.92402×10^{-04}	8.91745×10^{-04}	9.734×10^{-05}	1.00
RMSE Model of PV module						
CPSO	2.46278×10^{-03}	2.48025×10^{-03}	3.69473×10^{-03}	2.49627×10^{-03}	2.246×10^{-05}	0.87
HSA	2.45923×10^{-03}	2.46032×10^{-03}	3.73462×10^{-03}	2.48991×10^{-03}	5.723×10^{-05}	0.82
ABSO	2.41724×10^{-03}	2.41724×10^{-03}	2.52377×10^{-03}	2.43572×10^{-03}	2.175×10^{-05}	1.00
SA	2.42401×10^{-03}	2.43749×10^{-03}	3.52741×10^{-03}	2.49831×10^{-03}	2.053×10^{-05}	0.92
DET	2.41724×10^{-03}	2.41724×10^{-03}	2.41926×10^{-03}	2.42472×10^{-03}	2.946×10^{-09}	1.00

Table 10 for single diode model, double diode model, and model of PV module. RMSE is used to measure the fitness between the experimental data and the simulated data. The minimal, maximal, median, mean and standard deviation for the RMSE performance, over 100 trails are presented in Table 10. In addition, the significance of RMSE between two algorithms has been studied the Wilcoxon signed rank test. The test is carried out using the online test tool [49]. The success rate indicates that the DET performs better than other methods.

4.5. Comparison with other methods

The results of different parameter extraction methods with different performance criteria for single diode model, double diode model, and PV module are described in Tables 2–4 respectively. For the RMSE performance, the IAE and RE are calculated for 26 different measurements. Based on the results shown in Figs. 8–14 and Tables 2–4, it can be indicated that:—

- In terms of RMSE, the proposed DET method consistently obtains the best results compared with other parameter extraction techniques in all the cases. In addition, the IAE and RE values of DET are smaller compared to other methods such as HSA and ABSO techniques.

- When comparing the proposed method with different PV cells and modules, it is indicated that the results replicate the effectiveness and efficiency of the proposed method.
- With respect to convergence speed, it is listed in Figs. 6 and 9, the DET method converges the fastest, followed by ABSO, HSA, GA, and CPSO. DET is successively converging and provides an optimal solution during the whole parameter extraction process.

5. Conclusion

In this paper, a novel parameter extraction technique called DET is used for solar cell models. The proposed technique offers several advantages such as accuracy of solution, speed of convergence and balance between exploration and exploitation. The DET method is applied to different solar cell models such as a single diode, double diode, and PV modules for extracting the parameters. Comparisons are performed with other parameter extraction techniques such as ABSO, CPSO, HSA, SA, PS, OIS, and DAB, and the proposed method performs better than the other techniques. The feasibility of the DET technique is verified by experimental I-V data set of multi-crystalline and monocrystalline solar cells and modules. Comparing RMSE of the proposed method with other extraction methods, DET produces the best results consistently for all the cases. The proposed technique is accurate and shows rapid convergence to the solution. Therefore the proposed method provides an alternate method to parameter extraction for solar cell models.

References

[1] W. Zhou, H. Yang, N. Fang, A novel model for photovoltaic array performance prediction, Appl. Energy 84 (12) (2007) 1187–1198.
[2] J.S. Golden, J. Carlson, K.E. Kaloush, P. Phelan, A comparative study of thermal and radiative impacts of photovoltaic canopies on pavement surface temperatures, Sol. Energy 81 (2007) 872–883.
[3] B. Amrouche, A. Guessoum, M. Belhamel, A simple behavioural model for solar module electric characteristics based on the first order system step response for MPPT study and comparison, Appl. Energy 91 (1) (2012) 395–404.
[4] F. Khan, S.H. Baek, Y. Park, J.H. Kim, Extraction of diode parameters of silicon solar cells under high illumination conditions, Energy Convers. Manage. 76 (2013) 421–429.
[5] G. Walker, Evaluating MPPT converter topologies using a MATLAB PV model, J. Electr. Electron Eng. Aust. 21 (1) (2001) 1–6.
[6] C.T. Sah, R.N. Noyce, W. Shockley, Carrier generation and recombination in P-N junctions and P-N junction characteristics, Proc. IRE 45 (1957) 1228–1243.
[7] A. Jain, A. Kapoor, Exact analytical solutions of the parameters of real slar cells using Lambert W-function, Sol. Energy Mater. Sol. Cells 81 (2) (2004) 269–277.
[8] M. Chegaar, G. Azzouzi, P. Mialhe, Simple parameter extraction method for illuminated solar cells, Solid State Electron. 50 (2006) 1234–1237.
[9] W. De Soto, S.A. Klein, W.A. Beckman, Improvement and validation of a model for photovoltaic array performance, Sol. Energy 80 (2006) 78–88.
[10] R. Gottschalg, et al., The influence of the measurement environment on the accuracy of the extraction of the physical parameters of solar cells, Meas. Sci. Technol. 10 (9) (1999) 796–804.
[11] K. Ishaque, Z. Salam, An improved modeling method to determine the model parameters of photovoltaic (PV) modules using differential evolution (DE), Sol. Energy 85 (2011) 2349–2359.
[12] X. Lingyun, S. Lefei, H. Wei, J. Cong, Solar cell parameter extraction using a hybrid genetic algorithm, in: Third International Conference on Measuring Technology and Mechatronics Automation, 2011, pp. 306–309.
[13] J.A. Jervase, et al., Solar cell parameter extraction using genetic algorithm, Meas. Sci. Technol. 12 (2001) 1922.
[14] E.Q.B. Macabebe, C.J. Sheppard, E.E. Van Dyk, Parameter extraction from I-V characteristics of PV devices, Sol. Energy 85 (2011) 12–18.
[15] S. Asif, Solar cell modeling and parameter optimization using simulated annealing, J. Propul. Power 24 (2008) 1018–1022.
[16] M. Zagrouba, A. Sellami, M. Bouaicha, M. Ksouri, Identification of PV solar cells and modules parameters using the genetic algorithm: application to maximum power generation, Sol. Energy 84 (5) (2010) 860–866.
[17] M. Ye, X. Wang, Y. Xu, Parameter extraction of solar cells using particle swam optimization, J. Appl. Phys. 105 (9) (2009) 094502.
[18] W. Huang, C. Jiang, L. Xue, D. Song, Extracting solar cell model parameters based on chaos particle swam optimization, in: Proceedings of International Conference on Electric Information and Control Engineering (ICEICE), 2011, pp. 398–402.
[19] K. Ishaque, Z. Salam, S. Mekhilef, A. Shamsudin, Parameter extraction of solar photovoltaic modules using penalty-based differential evolution, Appl. Energy 99 (2012) 297–308.
[20] M. Ji, Z. Jin, H. Tang, An improved simulated annealing for solving the linear constrained optimization problems, Appl. Math. Comput. 183 (2006) 251–259.
[21] M. Ye, X. Wang, Y. Xu, An extraction method of solar cell parameters with improved particle swam optimization, J. Appl. Phys. 105 (2009) 1099–1104.
[22] L. Sandrolini, M. Artioli, U. Reggiani, Numerical method for the extraction of photovoltaic module double-diode model parameters through cluster analysis, Appl. Energy 87 (2010) 442–451.
[23] W. Wang, J.-M. Wu, J.-H. Liu, A particle swarm optimization based on chaotic neighborhood search to avoid premature convergence, in: Third International Conference on Genetic and Evolutionary, Computing, 2009, pp. 633–636.
[24] K. Ishaque, Z. Salam, H. Taheri, Simple, fast and accurate two-diode model for photovoltaic modules, Sol. Energy Mater. Sol. Cells 95 (2011) 586–594.
[25] M.A. Semenov, D.A. Terkel, Analysis of convergence of an evo- lutionary algorithm with self-adaptation using a stochastic Lyapunov function, Evol. Comput. 11 (4) (2003) 363–379.
[26] S. Das, P. Suganthan, Differential evolution: a survey of the state-of-the-art, IEEE Trans. Evol. Comput. 15 (1) (2011) 4–31.
[27] E. Mezura-Montes, J. Velazquez-Reyes, C.A. Coello Coello, A comparative study of differential evolution variants for global optimization, in: Proceedings of the 8th Annual Conference on Genetic and Evolutionary Computation, GECCO2006, 2006, pp. 485–492.
[28] J. Tvrdik, Adaptation in differential evolution: a numerical comparison, Appl. Soft Comput. 9 (2009) 1149–1155.
[29] J. Cubas, S. Pindalo, M. Victoria, On the analytical approach for modeling photovoltaic systems behavior, J. Power Sources 247 (2014) 467–474.
[30] H.M. Tian, F. Mancilla David, K. Ellis, E. Muljadi, P. Jenkins, A cell-to-module-to-array detailed model for photovoltaic panels, Sol. Energy Mater. Sol. Cells 86 (9) (2012) 2695–2706.
[31] K. Ishaque, Z. Salam, H. Taheri, A comprehensive MATLAB simulink PV system simulated with partial shading capability based on two-diode model, Sol. Energy 85 (2011) 2217–2227.
[32] Y.-H. Ji, J.-G. Kim, S.-H. Park, C.-Y. Won, C-language based PV array simulation technique considering effects of partial shading, in: IEEE International Conference on Industrial Technology (ICIT), 2009, pp. 1–6.
[33] R. Storn, K. Price, Differential evolution-a simple and efficient heuristic for global optimization over continuous spaces, J. Glob. Optim. 11 (1997) 341–359.
[34] K.V. Price, An introduction to differential evolution, in: D. Corne, M. Dorigo, M. Glover (Eds.), New Ideas in Optimization, McGraw-Hill, London, 1999, pp. 79–108.
[35] J. Best, S. Greiner, B. Boskovic, M. Mernik, V. Zumer, Self adapting control parameters in differential evolution: a comparative study in numerical benchmark problem, IEEE Trans. Evol. Comput. 10 (6) (2006) 646–657.
[36] J. Liu, J. Lampinen, A fuzzy adaptive differential evolution algorithm, Soft Comput. 9 (6) (2005) 448–462.
[37] V. Quaschning, R. Hanitsch, Numerical simulation of current-voltage characteristics of photovoltaic systems with shaded solar cells, Sol. Energy 56 (1996) 513–520.
[38] J. Zhang, A.C. Sanderson, JADE: adaptive differential evolution with optional external archive, IEEE Trans. Evol. Comput. 13 (5) (2009) 945–958.
[39] J. Zhang, A.C. Sanderson, Adaptive Differential Evolution: a Robust Approach to Multimodal Problem Optimization, Springer-Verlag, Berlin, 2009.
[40] J.H. Mathews, Numerical Methods for Computer Science, Engineering and Mathematics, Prentice Hall, NJ, 1987.
[41] M.R. AlHajri, M.F. ALHajri, K.M. El-Naggar, A.K. Al-Othman, A new estimation approach for determining the I-V characteristics of solar cells, Sol. Energy 85 (7) (2011) 1543–1550.
[42] A. Askarzadeh, A. Rezazadeh, Artificial bee swarm optimization algorithm for parameters identification of solar cell models, Appl. Energy 102 (2013) 943–949.
[43] K.M. El-Naggar, M.R. AlRashidi, Al-Othman A.K. AlHajri, Simulated annealing algorithm for photovoltaic parameters identification, Sol. Energy 86 (1) (2012) 266–274.
[44] M.R. AlRashidi, M.F. AlHajri, K.M. El-Naggar, A.K. Al-Othman, A new estimation approach for determining thr I-V characteristics of solar cells, Sol. Energy 85 (7) (2011) 1543–1550.
[45] M. Chegaar, N. Nehaoua, A. Bouhemadou, Organic and inorganic solar cells parameters evacuation from single I-V plot, Energy Convers. Manag. 49 (2008) 1376–1379.
[46] K. Bouzidi, M. Chegaar, M. Aillerie, Solar cells parameters evaluation from dark I-V characteristics, Energy Procedia 18 (2012) 601–610.
[47] J. Brest, S. Greiner, B. Boskovic, M. Mernik, V. Zumer, Self-adapting control parameters in differential evolution: a comparative study on numerical benchmark problems, IEEE Trans. Evol. Comput. 10 (6) (2006) 646–657.
[48] R. Boukenoui, R. Bradai, H. Salhi, A. Mellit, Modelling and simulation of photovoltaic strings under partial shading conditioned using Matlab/Simscape, in: IEEE 5th International Conference on Clean Electric Power (ICCEP), Italy, 2015, pp. 79–83.
[49] www.mathcracker.com/wilcoxon-rank-sum.php [last accessed : 22.02.16].